SCIENCE FOR GLASS PRODUCTION

UDC 666.1.031.2:662.612.324.001.42

ANALYTICAL ESTIMATE OF THE HEATING REGIME FOR A RECUPERATIVE GLASS-MELTING FURNACE

V. I. Kut'in,[1] S. N. Gushchin,[1] and Yu. V. Kryuchenkov[1]

Translated from Steklo i Keramika, No. 9, pp. 3 – 7, September, 1998.

The results of an analytical evaluation of the heat transfer processes in the working space of the furnace are presented. Four atomizers located under the nozzle of the burner are used for heating. The calculations are performed using a three-dimensional heat transfer zonal model for three variants of the thermal load distribution between the atomizers, as well as for heating of the furnace with natural gas (non-luminous flames).

The authors performed analytical calculations for the working space of direct-flow recuperative glass-melting furnaces with a double roof using a three-dimensional mathematical zonal model.

The analysis of previously obtained data [1 – 3] made it possible to improve the heating system in these furnaces, namely, to reduce to four the number of atomizers installed across the width of the working space of the chamber and redistribute the fuel rate, i.e., to increase the flow rate in the middle atomizers and decrease it in the outer atomizers [4]. Modification of the atomizer design (instead of the Shukhov design) ensured better atomization of the liquid fuel (primarily, mazut, and later on, kerosene) and made it possible to control the flame length to approximate it to the optimum length. All of this stabilized thermal operation of the furnace and improved its technical and economic parameters.

The experimentally found solutions required a corresponding theoretical basis and a search for further ways to improve of the thermal operation of the furnace. Therefore, it appeared advisable to use the mathematical instruments developed for the zonal calculation method [5] in the analysis of heat-transfer processes in the glass-melting tank of this type of furnaces.

Since symmetry is admissible for variations in the heat flows across the working space, in development of a three-dimensional model, the heat-transfer processes were analyzed in only one half of the furnace, since the melting area is conventionally divided along the center line into two halves by a mirror plane, and the resulting heat exchange between the two halves is equal to zero.

The scheme of the three-dimensional model of the gas space in the furnace (i.e., the space limited by the glass melt surface) is shown in Fig. 1. The working space is represented as a parallelepiped split into 8 estimated segments along the length, and into 4 estimated segments across the furnace width (from the lateral wall to the center line). The space between the furnace roofs was not considered, except for the part where the combustion products move under the second roof. Thus, the working space of the furnace is considered as 192 volume and surface zones, including: 68 volume zones of the gas space, including the working chamber; 32 surface zones of the glass melt; 32 surface zones of the roof; 16 surface zones of the end walls; 17 surface zones of the lateral

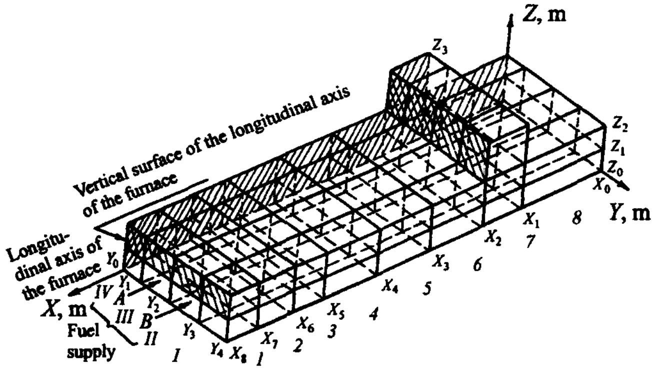

Fig. 1. Scheme of a zonal model of the working space of the furnace. *1 – 8*) Numbers of estimated zones along the furnace length; *I – IV*) same, across the furnace width; X_i, Y_i, Z_i) coordinates of zonal borders (Table 1); *A* and *B*) installation sites of the atomizers: middle and outer atomizer, respectively.

[1] Ural State Technical University, Ekaterinburg, Russia.

0361-7610/98/0910-0267$20.00 © 1999 Kluwer Academic/Plenum Publishers

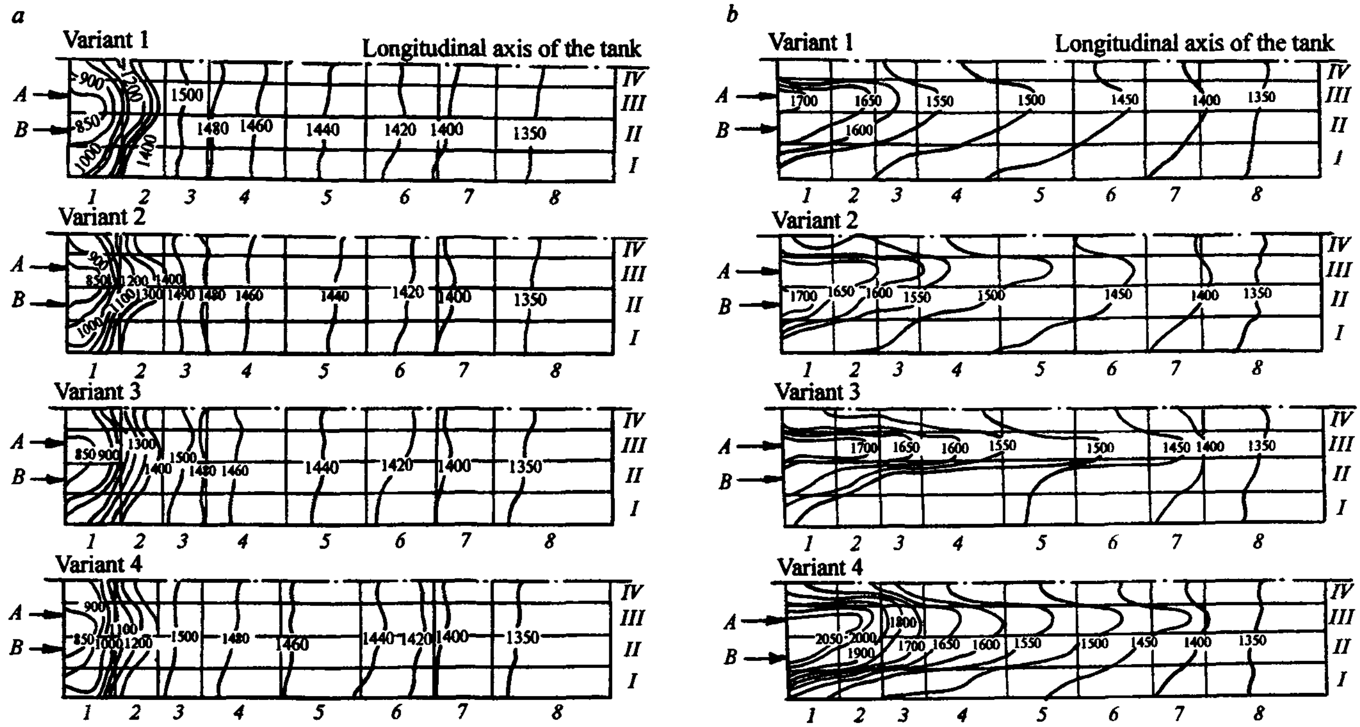

Fig. 2. Isotherms of the gas layer under the roof of the working space of the furnace (*a*) and above the melt surface (*b*) for different variants of fuel distribution between atomizers. *1 – 8*) numbers of estimated zones along the furnace length; *I – IV*) same, across the furnace width; *A*) axis of the middle flame; *B*) axis of the outer flame; figures on the lines) temperature, °C.

walls; and 25 mirror surface zones (in Fig. 1 they are shaded). The zone border coordinates are shown in Table 1.

All calculations were performed on an ES-1033 computer. The fuel (kerosene) flow rate used for heating amounted to 420 liter/h (344.4 kg/h) with combustion heat of 43.08 MJ/kg. The air heating temperature was 850°C, the air rate coefficient was 1.1.

The length of the flames was assigned based on previously obtained results [4] in determining the optimum length for groups of flames ensuring uniformity of descending heat flows. Thus, for the conditions of the furnace considered in the model, the flame length was taken to be equal to 2.525 m for middle atomizers *A*, and 1.725 m for outer atomizers *B*.

The degree of burn-out of fuel along the length of the flames, the air inflow in them, as well as the absorption coefficients for the soot particles and combustion products were calculated in advance according to the method described in [6]. Table 2 shows the absorption coefficients calculated for gases K_g and soot particles K_s in the flame spread areas. The other zones of the gas space were considered to be filled with combustion products for which K_g varied from 0.05 to $0.12\ m^{-1}$.

The coefficients of convective heat transfer near the glass melt surface were specified from 15 to 8 $W/(m^2 \cdot K)$ along the furnace length and 8 $kW/(m^2 \cdot K)$ for the brickwork surface.

Based on the data for the glass melt temperature measured by an immersion thermocouple [5], the following glass melt temperatures were specified in the calculation for sites

TABLE 1

Border coordinates, m	Distance from the reference point to zonal borders, m, according to the numbers of the respective borders							
	1	2	3	4	5	6	7	8
X_i	2.035	3.086	4.494	5.902	7.310	8.110	9.035	9.825
Y_i	0.304	0.911	1.518	2.125	–	–	–	–
Z_i	0.480	0.960	2.200	–	–	–	–	–

TABLE 2

Flame	Absorption coefficient, m^{-1}		
	K_g	K_s	$K_g + K_s$
Middle flame:			
*1**	0.0948	0.8266	0.9214
2	0.1399	0.1903	0.3302
3	0.1702	0.0310	0.2012
Outer flame:			
1	0.1710	0.2180	0.3890
2	0.1854	0.0934	0.2788

* *1 – 3*) Numbers of estimated zones along the furnace length.

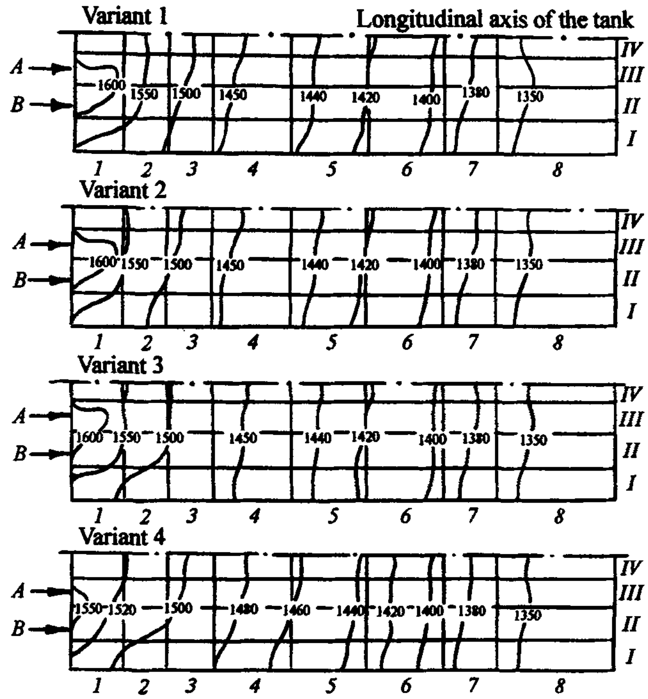

Fig. 3. Isotherms of the inner surface of the roof of the working space for different variants of fuel distribution between atomizers. Designations as in Fig. 2.

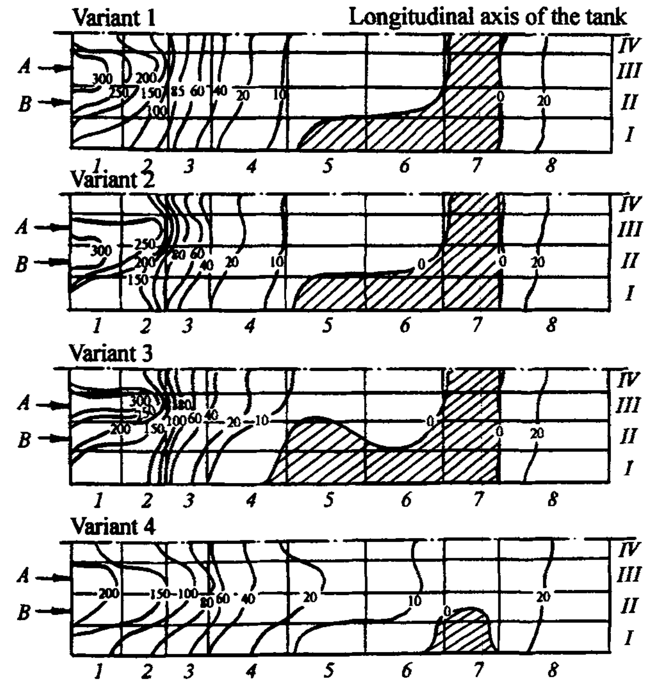

Fig. 4. Distribution of specific heat flow over the surface of the glass melt zones for different variants of fuel distribution between the atomizers. Designations as in Fig. 2; digits on the lines) specific heat absorption (kW/m^2).

1 – 8, respectively: 1420, 1435, 1440, 1460, 1450, 1420, 1400, and 1330°C.

The analytical estimate of external heat transfer in the glass-making tank in the conditions described above was performed for different variants of fuel distribution between the atomizers (Table 3). Variant 1, which represents the existing thermal conditions in the functioning furnace, is the basic variant.

Figures 2 – 4 show the results of the calculation of temperature fields for the surface and volume zones of the glass-melting tank and the absorption density of the melt surface.

In order to assess the adequacy of the model, the estimated values of the internal surface temperatures of the lateral walls and the roof were correlated with the readings of the stationary sensors installed in the furnace. On the whole, the nature of the temperature distribution over the internal surface of the brickwork corresponded to the specific heat process in the gas space: the maximum temperature values along the furnace length fully agree with the existing technological zones (melting area: sites *1 – 3*; clarification area: sites *4*, *5*; cooling area: sites *6*, *7*; working tank area: site *8*). Thus, the readings of the radiation pyrometers sighted to the bottom of the carbofrax barrels installed on the internal surface of the lateral wall of the furnace exceeded the estimated temperature values by no more than 30°C. The estimated temperature of the smoke at the transition site under the second roof amounted to 1384 – 1418°C and differed insignificantly from the actual measurement results (the temperature registered by the aspirating thermocouple in this section of the furnace was equal to 1396 – 1418°C).

In the same way, the calculations of the gas space temperature sufficiently agreed with the readings of a stationary rod thermocouple suspended from the furnace roof in the working space above the working chamber of the tank (1350 and 1360°C : calculation and the measurement data, respectively).

Therefore, it can be stated that the model adequately reflects the heat exchange processes in an industrial furnace.

The analysis of the calculation results for variants 1 – 3 indicates that the nature of the temperature fields differs insignificantly in all cases. The highest nonuniformity is exhibited by the temperature fields of the gas space in the first three estimated zones (the area of flame spread). As the com-

TABLE 3

Variant	Fuel distribution between atomizers, %	
	middle (*A*)	outer (*B*)
1(4)*	30	20
2	25	25
3	40	10

* Variant 4 corresponds to the combustion of gas fuel in the absence of luminous soot particles in the flame (non-luminous flame).

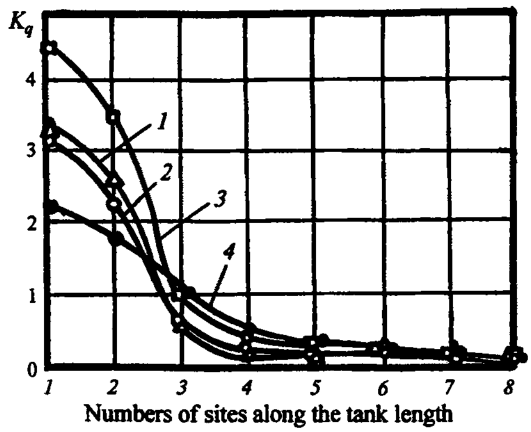

Fig. 5. Changes in the nonuniformity coefficient of specific heat flow K_q directed to the glass melt surface versus length of the working space of the furnace. *1 – 4*) Variants of fuel distribution between atomizers (Table 3).

bustion products migrate, the temperature fields across the furnace width are leveled, and this primarily happens in the upper layers of the gas space (under the roof, Fig. 2*a*), where starting with estimated zone 3, the temperature distribution across the gas space is virtually uniform.

In the lower layers of the gas space (near the glass melt surface, Fig. 2*b*), substantial nonuniformity of the temperature across the furnace width is maintained along the entire length of the tank. At the same time, the maximum temperature values in each estimated zone along the furnace length are observed along the middle flame axis, and the minimum values are registered near the brickwork surface. The temperature difference across the width varies from 180°C (first estimated zone) to 36°C, and in the end of the melting part of the tank the temperature field is virtually uniform.

The maximum temperature along the length of the lower part of the gas space is registered in the first estimated zone. The temperature gradient along the furnace length decreases in the direction of migration of the combustion products. In the upper zones of the gas space, the maximum temperature is registered in the third zone, which is due to the effect of relatively "cool" air flowing in from the recuperator. The temperature level of the upper zones is significantly lower than in the zones adjacent to the melt surface; the temperature gradient along the melting part is significantly lower as well.

The temperature field of the roof surface (Fig. 3) exhibits sufficiently high uniformity across the width of the working space. Noticeable nonuniformity of the temperature field is observed only in the first few estimated zones: in the part of the roof located above the luminous flames. The temperature of the roof along the furnace length decreases in the direction of migration of the combustion products. The roof temperatures do not exceed 1620°C, and the maximum is registered in estimated zone 1 above the middle flame. It points to the fact that the roof temperature allows for boosting the thermal operation of the furnace by increasing the overall heat load.

Significant nonuniformity in the specific heat absorption of the melt is observed in the first two estimated zones in the area of the luminous flames (Fig. 4). The nonuniformity of heat absorption across the furnace width decreases in the direction of migration of the combustion products. Both the value and the gradient of specific heat absorption decrease along the length of the melting space.

In the chilling area (estimated zones *6* and *7*) and near the lateral wall (zone *5*), heat inflow to the tank is virtually absent,

The experimental measurements indicated that the temperature of the glass melt surface significantly decreases between estimated zones *7* and *8*. This is due to the fact that the melt enters the working tank through the furnace neck from the cooler layers of the melting tank (according to the readings of the stationary thermocouple, the temperature of the glass melt in the bottom layers in front of the neck is equal to 1230°C). The positive heat absorption of the glass melt in the working tank derived from the calculations can be attributed to the longitudinal transfer of radiant heat from the high-temperature zones of the gas space and brickwork to the relatively low-temperature area of the glass melt surface.

The redistribution of the heat load across the width of the furnace and increase in the fuel rate of the middle atomizers (variant 3) produced noticeable deformation in the temperature field of the gas space, both above the melt and near the roof; the temperature difference across the width of the working space increased, the high-temperature region shifted towards the middle atomizer axis, and the extent of the high-temperature region along the axis of the middle atomizer increased. However, these changes can be seen only in the first three estimated zones (Fig. 2, variant 3). The temperature field of the inner surface of the roof was deformed in the same direction (Fig. 3).

An increase in the fuel rate of the middle atomizers substantially affected the specific heat flow distribution over the melt surface. The maximum heat absorption region perceptibly shifted towards the working space axis and extended a little toward the cooling area. At the same time, the area of the melt surface which does not absorb heat increased, especially near the lateral wall.

It should be noted that such redistribution of heat absorption of the melt will inevitably produce an increase in the convective flows of the glass melt in the melting tank sections, which is particularly undesirable for the first part of the tank, since as a consequence, incompletely melted batch can penetrate into the bottom layers of the melt. This can impair the quality of the finished product which will be insufficiently melted. Therefore, redistribution of the heat load toward a higher fuel flow rate of the middle atomizers should be considered advisable.

The relative characteristics of the heat absorption fields of the melt will be given using the coefficient of specific heat

flow nonuniformity K_q, which is the ratio of the maximum heat flow density in a particular estimated zone q_{max} to its mean integral value for the melt surface q_{mean}

$$K_q = \frac{q_{max}}{q_{mean}},$$

where $q_{mean} = \int_0^x \bar{q}_n \, dx/x$; $\bar{q}_n = \int_0^y q_i \, dy/y$; q_i is the specific heat flow directed to the ith surface zone of the melt; y is the current coordinate across the working space from the furnace axis in the nth estimated zone; x is the current coordinate along the length of the working space starting with the working chamber.

The change in the coefficients of nonuniformity of the heat flow density field along the furnace length for the analyzed variants of the heat load distribution between the atomizers is shown in Fig. 5. The highest degree of nonuniformity is exhibited by the density field in the first estimated zones along the length of the tank, and the nonuniformity of the heat absorption field increases as the heat load is shifted toward the working space axis.

The problem of the luminosity of the flames arises in the context of possible conversion of the furnace to natural gas fuel, which in combustion exhibits weak luminosity unless special measures are taken. The calculation of the heat transfer processes was performed for the same conditions as in Variant 1, but the absorption coefficients of the volume zones were determined for the combustion of gas fuel, i.e. in the absence of luminous particles in the flame. The calculation results presented in Figs. 2 – 5 correspond to variant 4.

The temperatures and their gradient in the gas layer near the melt surface became significantly higher (Fig. 2*a*). The temperature field of the gas layer under the roof varied insignificantly (Fig. 2*b*). This is due to a substantial decrease in the emitting properties of the flame due to a decrease in the degree of blackness of the flame.

The temperature of the roof surface slightly decreased in the foremost part of the furnace and increased in the middle part, which caused some leveling of the temperature field along the length of the working space (Fig. 3).

The decrease in the flame luminosity in the case of gas heating produced a decrease in the level of heat absorption in the initial zones and a slight increase in the middle part of the furnace due to the higher temperatures of the gas space and the roof in this area. The segment of zero heat absorption in the cooling area became significantly less, and virtually nothing changed in the working part of the tank.

Among the four variants analyzed, the highest degree of uniformity of the heat absorption field in the initial segments of the tank was exhibited by the gas heating variant (Fig. 5, curve *4*). Starting with zone 3, gas heating does not offer advantages in heat flow uniformity over kerosene heating.

It should be noted that while the integral indicators of the thermal efficiency of the furnace in the case of kerosene heating differed insignificantly in all variants of thermal load distribution between the atomizers, a decrease in the flame luminosity (Variant 4) did not affect these parameters either. The overall heat absorption of the melt decreased by approximately 1% compared to Variant 1 (the furnace efficiency decreased from 39.21 to 38.46%), and the temperature of the exhaust smoke in the working space increased slightly (by 6°C). This is due to the fact that the high-temperature region of the luminous flames occupies a relatively small share of the working space volume: the flame length does not exceed 0.25 of the tank length.

To conclude, note that the authors established the fact of the positive effect of redistribution of the thermal load toward the middle atomizers on the heat exchange processes in tank furnaces with transverse direction of the flame.

REFERENCES

1. S. N. Gushchin, V. P. Kut'in, N. I. Kokarev, et al., "Study of the thermal operation of the recuperative glass-melting furnace," *Steklo Keram.*, No. 4, 15 – 17 (1978).
2. S. N. Gushchin, V. Ya. Dzyurer, V. B. Kut'in, et al., "Improvement of thermal operation of the recuperative glass-melting furnace," *Steklo Keram.*, No. 12, 6 – 8 (1979).
3. S. N. Gushchin, V. B. Kut'in, A. A. Zeibots, et al., "Study of heat flows in the working space of the tank furnace," *Steklo Keram.*, No. 2, 6 – 8 (1980).
4. T. Ya. Dantsis, A. A. Zeibots, S. N. Gushchin, et al., "An improved heating system for small glass-melting furnaces with a new burner device," *Steklo Keram.*, No. 8, 7 – 8 (1980).
5. S. N. Gushcin, V. B. Kut'in, B. A. Fetisov, et al., "Measurement of the temperature of the glass melt surface in tank furnaces," *Steklo Keram.*, No. 11, 15 – 17 (1985).
6. V. G. Lisienko, *Intensification of Heat Exchange in Flame Furnaces* [in Russian], Metallurgiya, Moscow (1979).